https://doi.org/10.4047/jap.2026.18.1.55

Effect of scan body geometric configuration and library design on digital implant impression accuracy

Hong Seok Moon[1], Ahreum Choi[2], Kyung Chul Oh[1], Minji Sun[3], Jaeyoung Kim[1]*

[1]Department of Prosthodontics, Yonsei University College of Dentistry, Seoul, Republic of Korea
[2]Department of Dental Industry, Yonsei University College of Dentistry, Seoul, Republic of Korea
[3]Department of Prosthodontics, Ewha Womans University, Seoul, Republic of Korea

ORCID
Hong Seok Moon
https://orcid.org/0000-0001-8118-8145
Ahreum Choi
https://orcid.org/0009-0004-4752-9080
Kyung Chul Oh
https://orcid.org/0000-0003-4584-2597
Minji Sun
https://orcid.org/0000-0002-7402-2128
Jaeyoung Kim
https://orcid.org/0000-0002-2412-891X

PURPOSE. The purpose of this *in vitro* study was to evaluate how variations in scan body geometry, specifically body height and the length of the flat indexing surface (FIS), affect linear and angular accuracy when combined with truncated or full-geometry library files. **MATERIALS AND METHODS.** Nine scan body geometries were fabricated by combining three body heights (4, 5, and 6 mm) with three FIS lengths (1, 2, and 3 mm). Digital impressions were superimposed onto truncated or full-geometry library files. Linear deviation (ΔD) and angular deviation (ΔA) were calculated by comparing aligned scan bodies with coordinate measuring machine references. Linear and angular deviations were compared between library types using the Mann–Whitney U test, and differences among body heights and FIS lengths were evaluated using the Kruskal–Wallis test with Dunn's post-hoc test (α = .05). **RESULTS.** Linear deviation remained within a comparable range, and most geometry–library comparisons did not show a significant difference from body height, FIS length, or library morphology (P > .05). Angular deviation demonstrated geometry-dependent behavior, increasing only in the 4-mm body paired with larger FIS lengths, particularly when full-geometry libraries were used. No significant angular differences were observed in the 5-mm or 6-mm body groups. **CONCLUSION.** Digital implant registration remained stable across most configurations. Shortened scan bodies performed reliably when FIS dimensions were preserved. Angular accuracy was more sensitive to geometry-library interactions, with truncated libraries improving stability. [J Adv Prosthodont 2026;18:55-66]

KEYWORDS
Intraoral scan; Scan body; Flat indexing surface; Short scan body; Accuracy

Corresponding author
Jaeyoung Kim
Department of Prosthodontics, Yonsei University College of Dentistry, 50-1 Yonsei-ro, Seodaemun-gu, Seoul 03722, Republic of Korea
Tel +82-2-2228-3160
E-mail jaeyoungkim@yuhs.ac

Received November 26, 2025 / **Last Revision** January 18, 2026 / **Accepted** January 29, 2026

This research was supported by the Yonsei University College of Dentistry Fund (6-2022-0010).

INTRODUCTION

Digital technologies, including intraoral scanners and CAD-CAM systems, are

https://doi.org/10.4047/jap.2026.18.1.55

now integral to modern implant workflows, offering efficiency and reproducibility while supporting patient-centered treatment.[1,2] Among these components, the scan body plays a pivotal role by transferring the implant's three-dimensional spatial position into the virtual environment, thereby guiding the design and fabrication of the definitive prosthesis.[3-5] Because it serves as the initial reference for virtual registration, any deviation introduced at this stage may propagate through the entire prosthetic workflow. Inaccurate alignment between the scan body and its corresponding library may lead to positional errors, ultimately affecting implant angulation, platform location, prosthesis fit, occlusal harmony, and long-term stability.[6-9]

Although digital impressions have demonstrated sufficient accuracy for single-unit and short-span restorations, numerous variables, including scan body material, surface characteristics, spatial orientation, and the specific scanning protocol, continue to influence registration outcomes.[6,10,11] As such, the design characteristics of the scan body warrant further investigation, particularly regarding their influence on registration fidelity.

A wide range of strategies has been investigated to enhance the accuracy of intraoral scanning in implant dentistry, with particular focus on modifying scan body geometry.[6,9,10,12-14] Among these, several studies have addressed macroscopic design parameters, such as height, diameter, and mucosal exposure. Choi *et al*. reported that scan body exposure less than 3 mm was associated with increased angular deviation, particularly in posterior regions.[15] Gómez-Polo *et al*. found that reduced scan body height, especially in combination with angled implants, significantly compromised full-arch alignment.[16] Broader diameters have also been linked to better anti-rotational performance. Additionally, greater vertical exposure of the scan body, particularly in cases involving subgingivally placed implants, has been shown to improve landmark acquisition and reduce angular deviation.[15,17,18]

The dimensional behavior of a scan body during virtual alignment is influenced by its axial geometry,[19] which is defined primarily by two structural elements: the overall body height and the flat indexing surface (FIS) length. The FIS plays a critical role as the initial reference for virtual alignment, while the surrounding cylindrical geometry provides additional spatial constraints that help stabilize surface-based registration. Because these features guide how the registration algorithm interprets the object, their relative contributions determine the amount and diversity of geometric information available for digital matching.[20-22]

These same design elements, however, may also introduce limitations. A reduction in FIS length, particularly when combined with decreased scan body height, may limit the spatial information available for registration and thereby compromise alignment reliability. Conversely, excessive enlargement of the FIS may be undesirable, as an overly dominant indexing surface can diminish the contribution of the surrounding cylindrical geometry, reducing the geometric diversity needed for stable surface matching. This effect may be particularly relevant when full-body libraries are used, because disproportionate weighting of the FIS region can overshadow the broader geometric constraints provided by the scan body's overall contour.

In clinical situations such as limited interarch space, restricted mouth opening, or the need to remove the scan body before occlusal registration, shorter scan bodies would be advantageous. These practical considerations underscore the growing need for compact scan body designs that can remain in place throughout the clinical workflow without compromising accuracy. However, despite these demands, little is known regarding how reduced body height in combination with shortened FIS length affects digital registration, particularly when considered alongside differences in library geometry. To address this demand, the present study aimed to explore whether scan body length could be reduced while still maintaining reliable digital registration.

By systematically analyzing these design variables under controlled *in vitro* conditions, this study aims to determine the geometric relationships that yield the most stable registration performance and to identify the minimum scan body dimensions required to maintain acceptable accuracy. The findings may provide an evidence-based foundation for optimizing

shortened scan body designs in situations with limited interarch space or esthetic constraints.

Based on these considerations, the null hypotheses are:

1. The length relationship between body and FIS has no effect on digital implant registration accuracy.
2. The geometry of the library file (full vs. truncated) has no effect on digital implant registration accuracy.

MATERIALS AND METHODS

The experimental design and sequential workflow are illustrated in Fig. 1.

A reference model for evaluating scan body accuracy was fabricated by 3D printing a mandibular arch in which the right first molar region was intentionally left edentulous (Formlabs Form 3B+, Formlabs Inc., Somerville, MA, USA). A bone-level implant analog (GSTL400; Osstem Implant Co., Seoul, Korea) was subsequently inserted into the edentulous site at a depth of 3 mm below the gingival level. To establish a coordinate system and align the datasets, three silicon nitride ceramic balls (SBM-CER-4; Tsubaki Nakashima Co., Ltd., Nara, Japan) with a diameter of 4 mm were employed as reference markers. Two reference spheres were positioned on the buccal surfaces of the first and second molars, while one was positioned on the lingual surface of the second molar. All spheres and the implant analog were firmly fixed in place using an epoxy adhesive (VT-146; V-tech Co., Selangor, Malaysia) to prevent positional displacement during the scanning procedure (Fig. 2A).

A high-precision contact coordinate measuring machine (CMM; Spectrum II, Carl Zeiss, Oberkochen, Germany) was used to obtain the reference dataset for spatial deviation analysis. The master model was rigidly fixed to a dedicated CMM jig. Three precision ceramic spheres, previously mounted as fiducial markers, and the scan body (TSSBOS; Osstem Implant Co., Seoul, Korea) were probed to record their center coordinates in three dimensions (Fig. 2B).

To determine the platform-level coordinate of the scan body, the vertical distance between the top surface of the scan body and the implant platform was measured with the CMM. This value was subtracted from the measured top-surface coordinate to compute the platform center point.

The three-dimensional positional and directional data were then imported into a solid-modeling program (SolidWorks 2022; Dassault Systèmes, Waltham, MA, USA). These reference coordinates were applied to each model to visualize the spatial relationships between the scan body and the fiducial spheres and to establish the baseline dataset for

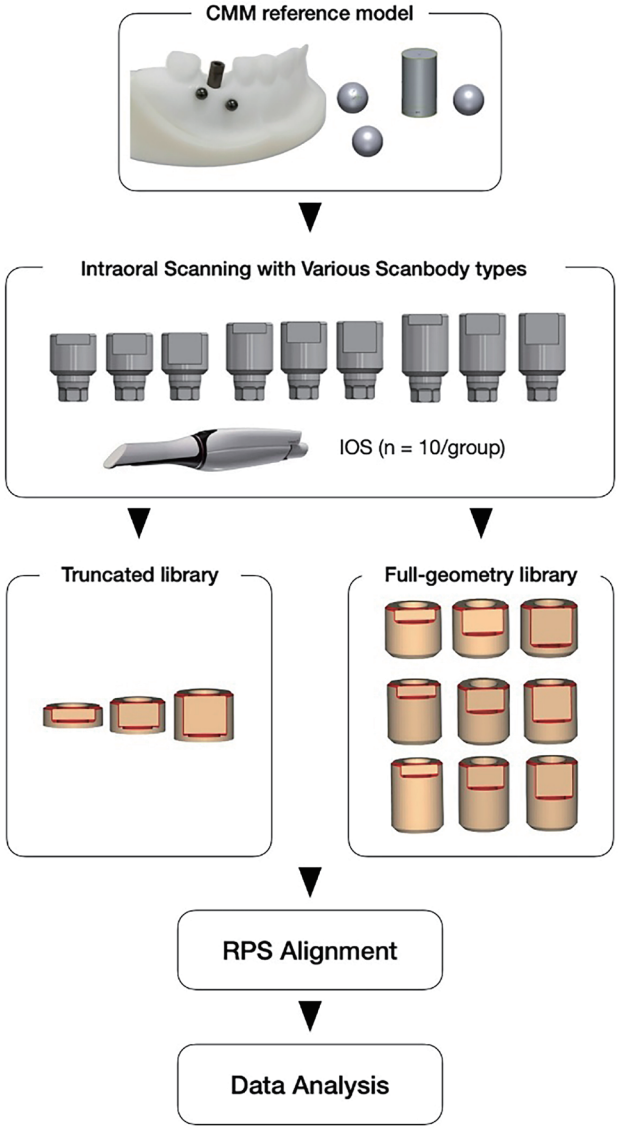

Fig. 1. Experimental workflow illustrating reference model acquisition, intraoral scanning, library configuration, and alignment steps.

https://doi.org/10.4047/jap.2026.18.1.55

Fig. 2. Experimental model and coordinate acquisition. (A) 3D-printed mandibular model with 4-mm ceramic spheres. (B) Coordinate measurement of scan body and spheres with contact CMM. (C) Three-dimensional reconstruction generated from mean CMM-derived coordinates.

subsequent deviation analysis (Fig. 2C).

Nine cylindrical scan body types were fabricated by combining three body lengths (4, 5, and 6 mm) with three flat indexing surface (FIS) lengths (1, 2, and 3 mm), yielding distinct geometric configurations (Fig. 3A). All scan bodies were milled from Ti-6Al-4V with high-precision computer numerical control (CNC) machining to minimize manufacturing deviations (ARUM 5X-200, Arum Europe GmbH, Frankfurt, Germany). A thin tungsten coating was applied to reduce light reflectivity during scanning.

The scan body library files were modeled using dental CAD software (ExocadDentalCAD v3.2; Exocad GmbH, Darmstadt, Germany) and categorized into two types based on geometry, while maintaining consistent segmentation parameters across all groups (Fig. 3B). The full-geometry library was designed to include the entire external structure of the scan body, extending from the upper surface to the implant platform, whereas the truncated library was limited to the region from the upper surface to 0.45 mm below the FIS reference level, providing surface information only for the indexing region to ensure complete preservation of the planar indexing geometry while excluding the apical cylindrical portion that contributes minimally to rotational constraint during initial alignment.

Each scan body was manually secured to the implant fixture using a calibrated torque of 20 N·cm with a torque wrench (TW-B30; Osstem Implant Co., Seoul, Korea), ensuring that FIS faced the buccal aspect. Intraoral scanning was performed (Trios 4, 3Shape, Copenhagen, Denmark) under controlled ambient conditions (23°C, 50% relative humidity). All scans followed the manufacturer-recommended scanning protocol for mandibular dentition. For each scan body-library combination, 10 scans were acquired, yielding a total of 180 scan datasets. All datasets were exported in standard tessellation language (STL) format.

The scan data and the corresponding library geometry were aligned in dental CAD software (ExocadDentalCAD v3.2; Exocad GmbH, Darmstadt, Germany) using a three-point alignment followed by best-fit matching. The virtual implant geometry was then exported as an STL file while maintaining the original coordinate system.

To analyze the positional and angular deviations of the platform centers, both the scan dataset and virtual implant geometry containing the original coordinate information were imported into Geomagic Control X (3D Systems, Inc.; Rock Hill, SC, USA). A reference cylinder was fitted to the implant geometry, and a plane was created on its coronal surface to identify the center of the circular platform. These coordinates were used to define the implant platform center point.

To enable quantitative comparison, both test and reference datasets were aligned within the same coordinate system using translation, rotation, and Reference Point System (RPS) alignment protocols. Linear deviation (ΔD) was calculated as the Euclidean

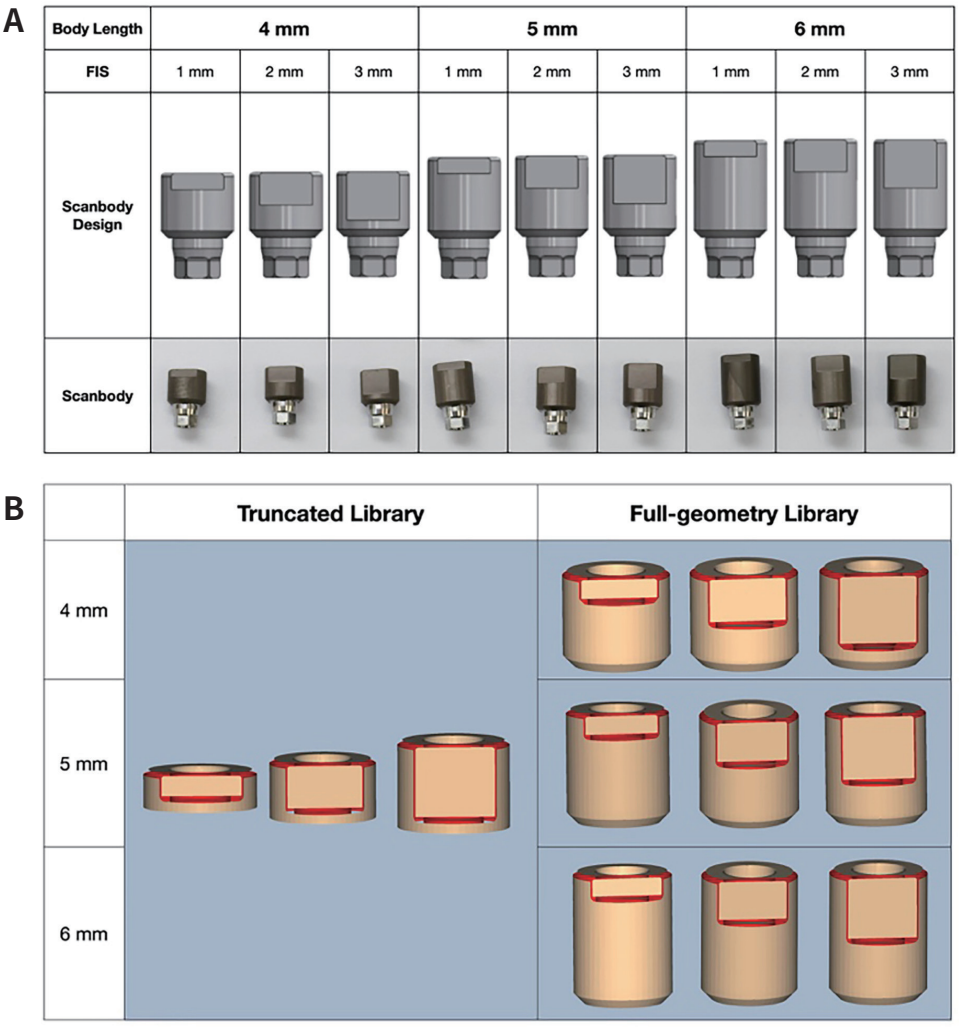

Fig. 3. Experimental scan body geometries and corresponding library designs. (A) Body height and flat indexing surface (FIS) combinations with fabricated scan bodies. (B) Truncated and full-geometry libraries for each configuration.

distance between the platform center points of the reference and test datasets. Angular deviation (ΔA) was computed as the angle between the implant axes derived from the fitted cylindrical features (Fig. 4).

The distribution of all outcome variables was assessed using the Shapiro-Wilk and Kolmogorov-Smirnov tests. Linear and angular deviations between the truncated and full library groups were compared using the Mann-Whitney U test. Within each body height group, differences according to FIS length were analyzed using the Kruskal-Wallis test, and the same test was applied to evaluate the effect of body height within each FIS length group. When significant differences were identified, pairwise comparisons were conducted using Dunn's post-hoc test. Statistical analyses were performed using a statistical software program (IBM SPSS Statistics, v29.0; IBM Corp., Armonk, NY, USA) and statistical significance was set at $\alpha = .05$.

RESULTS

A total of 180 scan datasets were analyzed. Linear deviation (ΔD) and angular deviation (ΔA) were assessed according to library morphology, FIS length, and body length.

https://doi.org/10.4047/jap.2026.18.1.55

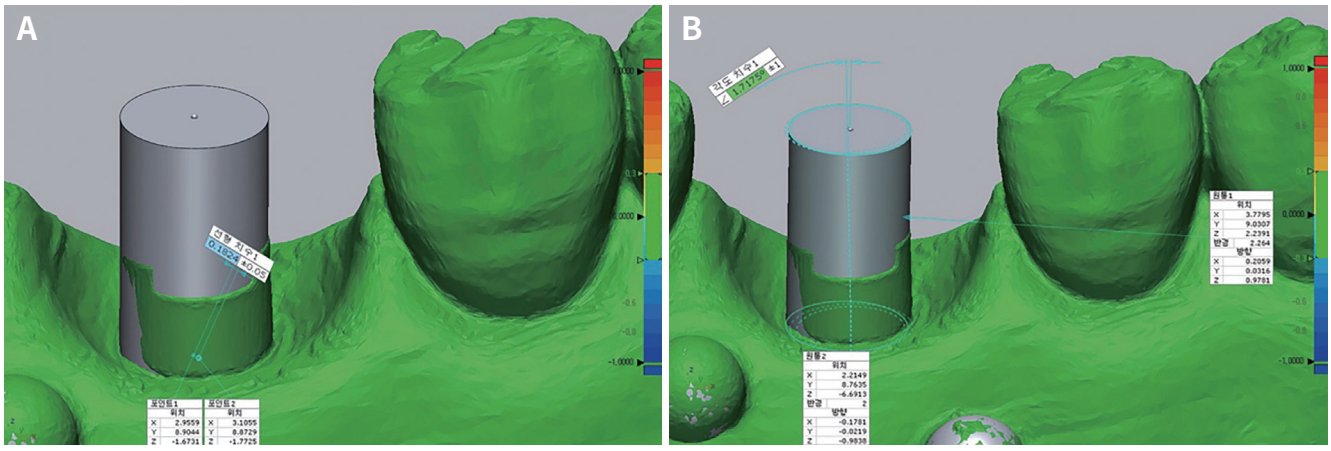

Fig. 4. Measurement of linear (ΔD) and angular (ΔA) deviations. (A) Linear deviation calculated between platform center points. (B) Angular deviation determined by comparing long axes of reference and test scan bodies.

Across all body-FIS configurations, linear deviation did not differ significantly between the truncated and full-geometry libraries. The only exception was the 4 mm body combined with a 2 mm FIS, in which the truncated library produced a lower linear deviation than the full-geometry library (P = .047). Angular deviation showed a similar pattern; most configurations demonstrated no significant differences between the two libraries. However, for the 4 mm body with 2 mm and 3 mm FIS configurations, the full-geometry library resulted in significantly greater angular deviation than the truncated library (P = .022 and P = .007, respectively). No significant differences related to library type were found in the 5 mm or 6 mm body groups (Table 1, Fig. 5).

Changes in FIS length did not significantly affect linear deviation in any of the 4-, 5-, or 6-mm body groups for either library type. In contrast, angular deviation was influenced by FIS length only when the body length was 4 mm. When the truncated library was used, the 3-mm FIS produced greater angular deviation than the 1-mm and 2-mm FIS. When the full-geometry library was used, both the 2-mm and 3-mm FIS resulted in greater angular deviation compared with the 1-mm FIS. No significant effects related to FIS length were observed in the 5-mm or 6-mm body groups (Table 2, Fig. 6).

When the truncated library was applied, linear deviation did not differ significantly among the 4-, 5-, and 6-mm bodies across all FIS configurations. With the full-geometry library, a significant difference was observed only in the 2-mm FIS configuration, where the 4-mm body produced greater linear deviation than the 6-mm body (P = .019). For angular deviation, body length had no significant influence when truncated libraries were used. However, with the full-geometry library, body length significantly affected angular deviation in both the 2-mm and 3-mm FIS configurations: the 4-mm body showed greater angular deviation than the 5-mm and 6-mm bodies in the 2-mm FIS configuration, and greater deviation than the 6-mm body in the 3-mm configuration (Table 3, Fig. 7).

Overall, linear deviation remained generally stable across most experimental conditions. Angular deviation increased selectively in short-body configurations paired with larger FIS lengths, particularly when full-geometry libraries were used.

DISCUSSION

This *in vitro* study examined how variations in scan body geometry, specifically body length and the length of the flat indexing surface (FIS), interact with different library morphologies to influence the accuracy of digital implant registration. A comprehensive range of geometry-library combinations was evaluated to determine whether shortened scan bodies could be used predictably in situations with limited interocclusal space or restricted mouth

Table 1. Linear deviation (ΔD) and angular deviation (ΔA) for each combination of body length and FIS length according to library type (truncated vs full-geometry)

	Body	FIS	Truncated	Full-geometry	*P* value
ΔD (mm)	4	1	0.202 ± 0.013	0.212 ± 0.010	.959
		2	0.208 ± 0.029	0.259 ± 0.069	.047
		3	0.207 ± 0.006	0.207 ± 0.007	.074
	5	1	0.211 ± 0.023	0.217 ± 0.047	.508
		2	0.198 ± 0.021	0.216 ± 0.063	.285
		3	0.204 ± 0.021	0.227 ± 0.073	.959
	6	1	0.233 ± 0.056	0.208 ± 0.027	.213
		2	0.215 ± 0.038	0.194 ± 0.015	.074
		3	0.216 ± 0.027	0.208 ± 0.022	.575
ΔA (°)	4	1	2.12 ± 0.41	2.23 ± 0.12	.959
		2	2.14 ± 0.45	2.98 ± 0.92	.022
		3	2.53 ± 0.05	2.47 ± 0.15	.007
	5	1	2.24 ± 0.27	2.32 ± 0.37	.959
		2	2.09 ± 0.17	2.18 ± 0.64	.646
		3	2.24 ± 0.30	2.52 ± 0.95	.575
	6	1	2.44 ± 0.62	2.07 ± 0.35	.203
		2	2.20 ± 0.37	1.93 ± 0.19	.074
		3	2.24 ± 0.39	2.05 ± 0.28	.169

Data are expressed as mean ± standard deviation.

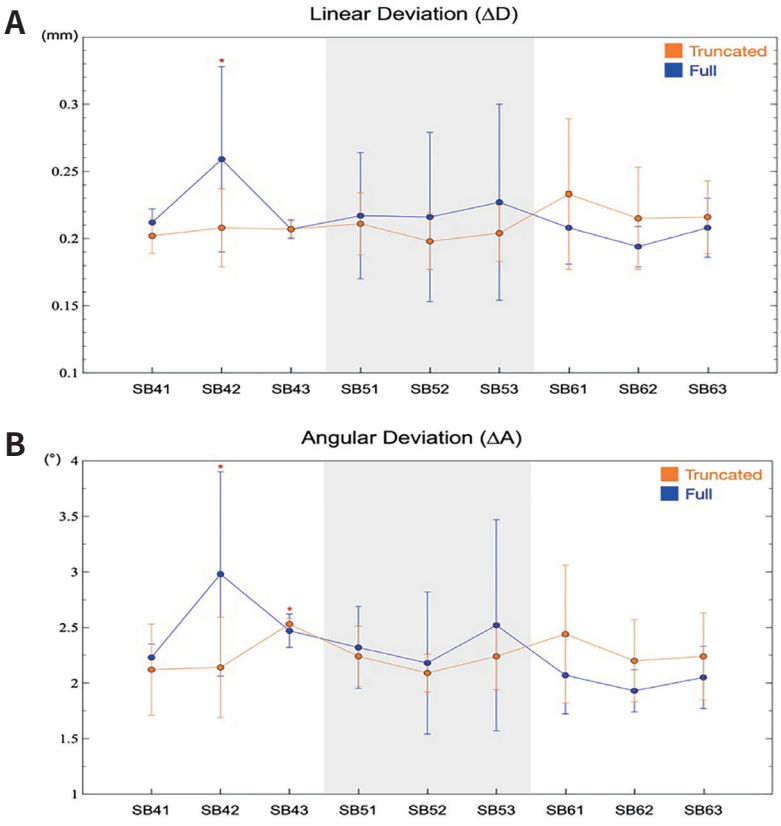

Fig. 5. Linear and angular deviation for truncated and full-geometry libraries across scan body configurations. (A) Linear deviation (ΔD). (B) Angular deviation (ΔA).

https://doi.org/10.4047/jap.2026.18.1.55

Table 2. Kruskal-Wallis test results for FIS length comparisons within each body height group, with Dunn's post-hoc pairwise tests applied for significant findings

	Truncated				Full-geometry			
	Body	*P*	Pairwise comparison (FIS length)	post hoc *P*	Body	*P*	Pairwise comparison (FIS length)	post hoc *P**
ΔD	4	.910			4	.073		
	5	.523			5	.817		
	6	.848			6	.303		
ΔA	4	< .001	1-2	1.000	4	.013	1-2	.038
			1-3	.002			1-3	.027
			2-3	.005			2-3	1.000
	5	.065			5	.061		
	6	.211			6	.209		

*Bonferroni adjustment
ΔD; Linear deviation, ΔA; Angular deviation

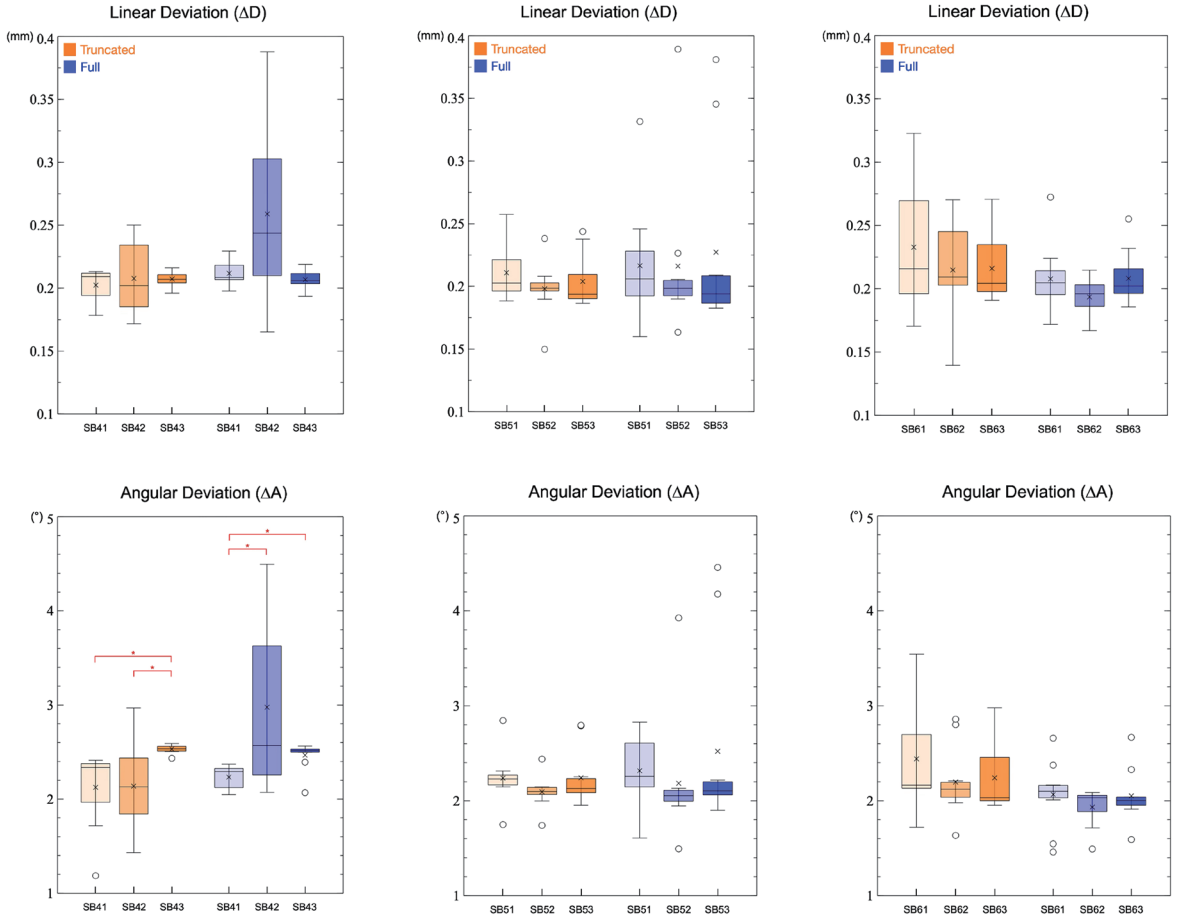

Fig. 6. Linear and angular deviation according to FIS length within each scan body length.

Table 3. Kruskal-Wallis test results for body height comparisons within each FIS length group, with Dunn's post-hoc pairwise tests applied for significant findings

	Truncated				Full-geometry			
	FIS	*P*	Pairwise comparison (Body length)	post hoc *P*	FIS	*P*	Pairwise comparison (Body length)	post hoc *P**
ΔD	1	.569			1	.493		
							4-5	.126
	2	.275			2	.019	4-6	.021
							5-6	1.000
	3	.141			3	.422		
ΔA	1	.869			1	.136		
							4-5	.020
	2	.910			2	< .001	4-6	.000
							5-6	.698
							4-5	.266
	3	.068			3	.006	4-6	.004
							5-6	.422

*Bonferroni adjustment
ΔD; Linear deviation, ΔA; Angular deviation

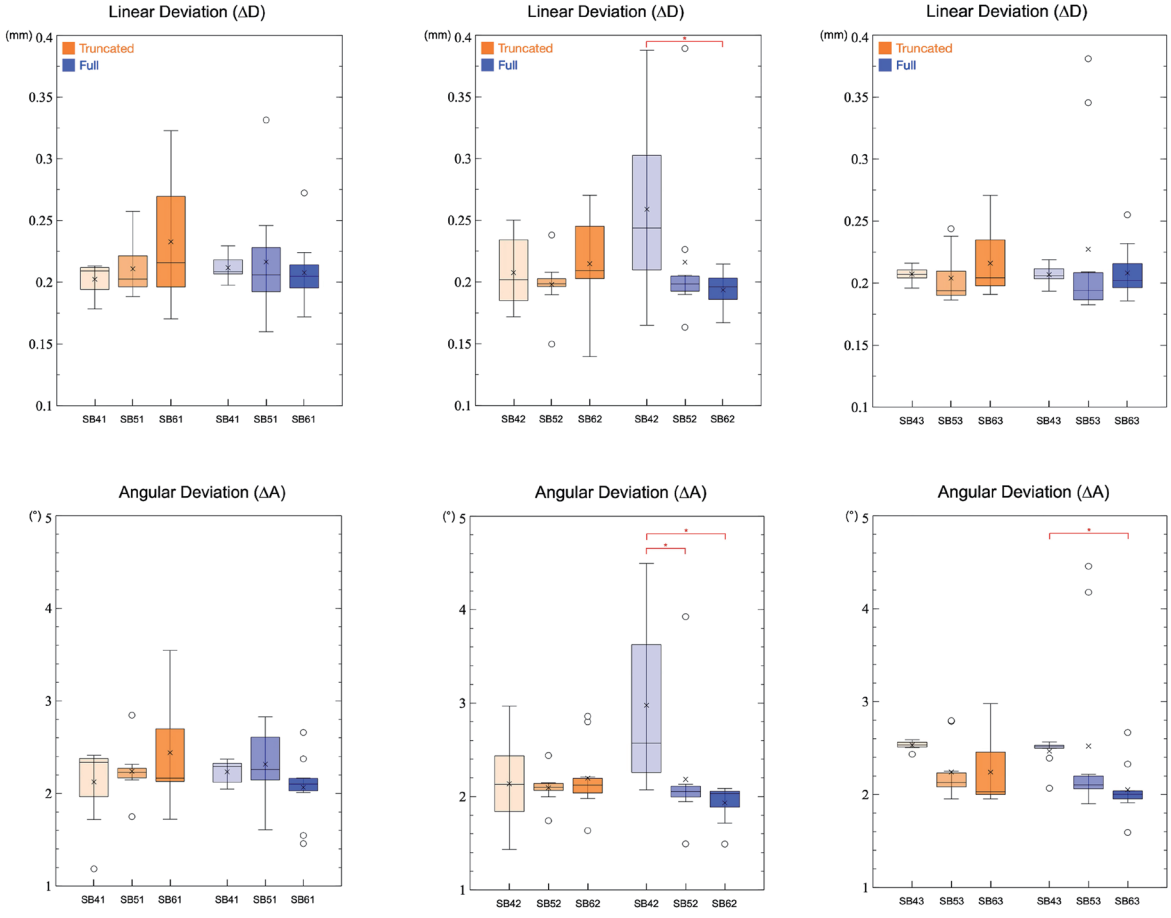

Fig. 7. Linear and angular deviation according to scan body length within each FIS length.

https://doi.org/10.4047/jap.2026.18.1.55

opening. Overall, most configurations demonstrated comparable linear and angular accuracy, suggesting that shortened scan bodies may be used safely when appropriate design parameters are preserved.

A key finding was that linear deviation remained generally stable across most geometry-library combinations. Neither body length nor FIS length caused significant changes in linear accuracy, and library morphology had only a minimal effect. These results indicate that the positional registration of the scan body platform is largely resilient to geometric reduction, provided that the FIS is present and adequately captured during scanning.

However, angular deviation exhibited a more geometry-dependent pattern. Increased angular deviation was observed only in configurations involving the 4-mm body paired with larger FIS lengths, particularly when full-geometry libraries were used. Wang *et al*. reported that, in intraoral scanning and partial surface registration, the effective overlap between the scanned surface and the corresponding library geometry may be reduced when portions of the scan body are obscured during scanning.[23] Under clinically relevant scanning conditions, the apical portion of the scan body is often partially covered by peri-implant soft tissue, resulting in incomplete capture of approximately 1 – 2 mm of the subgingival surface. When a full-geometry library is used in such situations, parts of the library geometry may lack corresponding scanned data, effectively reducing the true surface overlap available for registration and forcing the alignment algorithm to rely primarily on the limited supragingival region. In surface-based registration, this reduction in effective overlap increases rotational susceptibility because small local discrepancies within the remaining shared region can disproportionately influence the final alignment. Under these conditions, alignment may depend disproportionately on a small region of the surface geometry, resulting in greater rotational variability. In contrast, the truncated library, which concentrates alignment on the FIS region, may provide greater rotational stability even when the overall exposed geometry is limited. This selective pattern of increased angular deviation underscores that rotational accuracy is more sensitive than linear accuracy to geometry-library interactions, especially in short-body configurations.

These findings have several notable clinical implications. Shortened scan bodies have traditionally raised concerns regarding reduced indexing surface area and potential loss of rotational stability. However, the present results indicate that short scan bodies can achieve acceptable accuracy when the FIS length is maintained at approximately 1 mm and does not occupy an excessively large proportion of the exposed geometry. Notably, the increased angular deviation in the 4-mm condition was observed primarily with full-geometry libraries, suggesting that the error is related to reduced effective surface correspondence rather than short-body geometry alone. Accordingly, the observation that truncated libraries tended to produce lower angular deviation than full-geometry libraries in short-body configurations suggests that systems relying on simplified, FIS-centered alignment may offer practical advantages in situations with limited interocclusal space. These results may assist clinicians in selecting appropriate scan body configurations and library types when performing digital impressions for space-limited implant restorations.

Several limitations should be acknowledged. This study used a single implant system and was conducted under *in vitro* conditions that did not replicate soft-tissue interference or intraoral moisture. Although a high-precision reference system and a controlled scanning protocol were applied, only one intraoral scanner and a single segmentation approach were evaluated, and the findings may not fully generalize to other devices, library systems, or scanning environments.[24] Additional validation in multi-implant configurations or full-arch scenarios will be necessary to determine the broader applicability of these results.

Future research should investigate how these configuration-dependent effects manifest in clinical settings, particularly in the esthetic zone, where soft-tissue contours and limited labial exposure may further restrict the geometry available for registration, as well as in posterior regions with limited vertical clearance. The incorporation of alternative scanning devices, photogrammetry systems, and different library segmentation strategies may further elucidate

the interaction between scan body geometry and alignment algorithms. Computational modeling may also help define the dimensional thresholds at which scan body reduction begins to compromise rotational stability.

In summary, this study provides evidence that digital implant registration remains stable across most scan body configurations, with the exception of short-body geometries combined with disproportionately large FIS regions. Under these conditions, angular deviation increased, particularly when full-geometry libraries were used, whereas truncated libraries showed improved stability. These findings support the safe use of shortened scan bodies when appropriate FIS geometry is preserved and offer guidance for optimizing scan body design and library selection in digital implant workflows.

CONCLUSION

Within the limitations of this *in vitro* study, most scan body configurations demonstrated comparable positional and angular accuracy, supporting the safe use of shortened scan bodies in space-limited situations. Increased angular deviation was observed only when the 4 mm body was combined with a large FIS, indicating that an excessive FIS proportion may compromise rotational stability. Library morphology generally had little influence on accuracy; however, in short-body configurations, the full-geometry library produced greater alignment error, indicating that caution is required when it is used with limited exposed geometry. Overall, an FIS of approximately 1 mm appears sufficient, and these findings offer practical guidance for selecting scan body configurations and library designs in digital implant workflows.

REFERENCES

1. Joda T, Ferrari M, Gallucci GO, Wittneben JG, Brägger U. Digital technology in fixed implant prosthodontics. Periodontol 2000 2017;73:178-92.
2. Rekow ED. Digital dentistry: The new state of the art - Is it disruptive or destructive? Dent Mater 2020;36:9-24.
3. Mizumoto RM, Yilmaz B. Intraoral scan bodies in implant dentistry: a systematic review. J Prosthet Dent 2018;120:343-52.
4. Richert R, Goujat A, Venet L, Viguie G, Viennot S, Robinson P, Farges JC, Fages M, Ducret M. Intraoral scanner technologies: a review to make a successful impression. J Healthc Eng 2017;2017:8427595.
5. Pachiou A, Zervou E, Tsirogiannis P, Sykaras N, Tortopidis D, Kourtis S. Characteristics of intraoral scan bodies and their influence on impression accuracy: A systematic review. J Esthet Restor Dent 2023;35:1205-17.
6. Gómez-Polo M, Donmez MB, Çakmak G, Yilmaz B, Revilla-León M. Influence of implant scan body design (height, diameter, geometry, material, and retention system) on intraoral scanning accuracy: a systematic review. J Prosthodont 2023;32(S2):165-80.
7. Goodacre BJ, Goodacre SE, Goodacre CJ. Prosthetic complications with implant prostheses (2001-2017). Eur J Oral Implantol 2018;11 Suppl 1:S27-36.
8. Goodacre CJ, Bernal G, Rungcharassaeng K, Kan JY. Clinical complications with implants and implant prostheses. J Prosthet Dent 2003;90:121-32.
9. Michelinakis G, Apostolakis D, Nikolidakis D, Lapsanis G. Influence of different scan body design features and intraoral scanners on the congruence between scan body meshes and library files: an in vitro study. J Prosthet Dent 2024;132:454.e1-11.
10. Boz FD, Akca K. Comparison of fixed dental prostheses digitally fabricated using various scan bodies: a clinical study. J Adv Prosthodont 2025;17:70-82.
11. Mizumoto RM, Yilmaz B, McGlumphy EA Jr, Seidt J, Johnston WM. Accuracy of different digital scanning techniques and scan bodies for complete-arch implant-supported prostheses. J Prosthet Dent 2020;123:96-104.
12. Pan Y, Tsoi JKH, Lam WYH, Chen Z, Pow EHN. Does the geometry of scan bodies affect the alignment accuracy of computer-aided design in implant digital workflow: an in vitro study? Clin Oral Implants Res 2022;33:313-21.
13. Mohajerani R, Djalalinia S, Alikhasi M. The effects of scan body geometry on the precision and the trueness of implant impressions using intraoral scanners: a systematic review. Dent J (Basel) 2025;13:252.
14. Alvarez C, Domínguez P, Jiménez-Castellanos E, Arroyo G, Orozco A. How the geometry of the scan body

https://doi.org/10.4047/jap.2026.18.1.55

affects the accuracy of digital impressions in implant supported prosthesis. In vitro study. J Clin Exp Dent 2022;14:e1008-14.
15. Choi YD, Lee KE, Mai HN, Lee DH. Effects of scan body exposure and operator on the accuracy of image matching of implant impressions with scan bodies. J Prosthet Dent 2020;124:379.e1-6.
16. Gómez-Polo M, Sallorenzo A, Ortega R, Gómez-Polo C, Barmak AB, Att W, Revilla-León M. Influence of implant angulation and clinical implant scan body height on the accuracy of complete arch intraoral digital scans. J Prosthet Dent 2024;131:119-27.
17. Baranowski JH, Stenport VF, Braian M, Wennerberg A. Effects of scan body material, length and top design on digital implant impression accuracy and usability: an in vitro study. J Adv Prosthodont 2025;17:125-36.
18. Nam NE, Shin SH, Lim JH, Lee B, Shim JS, Kim JE. Accuracy of implant position reproduction according to exposed length of the scan body during optical scanning: an in vitro study. Appl Sci 2021;11:1689.
19. Pan Y, Dai X, Tsoi JK, Lam WY, Pow EH. Effect of shape and size of implant scan body on scanning accuracy: An in vitro study. J Dent 2025;152:105498.
20. He Y, Liang B, Yang J, Li S, He J. An iterative closest points algorithm for registration of 3D laser scanner point clouds with geometric features. Sensors (Basel) 2017;17:1862.
21. Huang T, Zhang D, Li G, Jiang M. Registration method for terrestrial LiDAR point clouds using geometric features. Optical Engineering. 2012;51:021114.
22. Gal R, Cohen-Or D. Salient geometric features for partial shape matching and similarity. ACM Transactions on Graphics (TOG). 2006;25:130-50.
23. Wang Y, Yan C, Feng Y, Du S, Dai Q, Gao Y. STORM: structure-based overlap matching for partial point cloud registration. IEEE Trans Pattern Anal Mach Intell 2023;45:1135-49.
24. Revilla-León M, Jiang P, Sadeghpour M, Piedra-Cascón W, Zandinejad A, Özcan M, Krishnamurthy VR. Intraoral digital scans: Part 2-influence of ambient scanning light conditions on the mesh quality of different intraoral scanners. J Prosthet Dent 2020;124:575-80.